VII Conference on Active Galactic Nuclei and Gravitational Lensing
July 20th - 24th, 2026

Analysis of the optical polarization of blazars based on long-term monitoring data

Shishkina E.V., Savchenko S.S., Morozova D.A., Jorstad S.G., Larionova E.G., Grishina T.S., Troitskiy I.S., Vasilyev A.A.
Saint Petersburg State University, St Petersburg, Russia
e.v.shishkina99@yandex.ru

21.07.2026

How can we probe the magnetic fields of blazar jets?

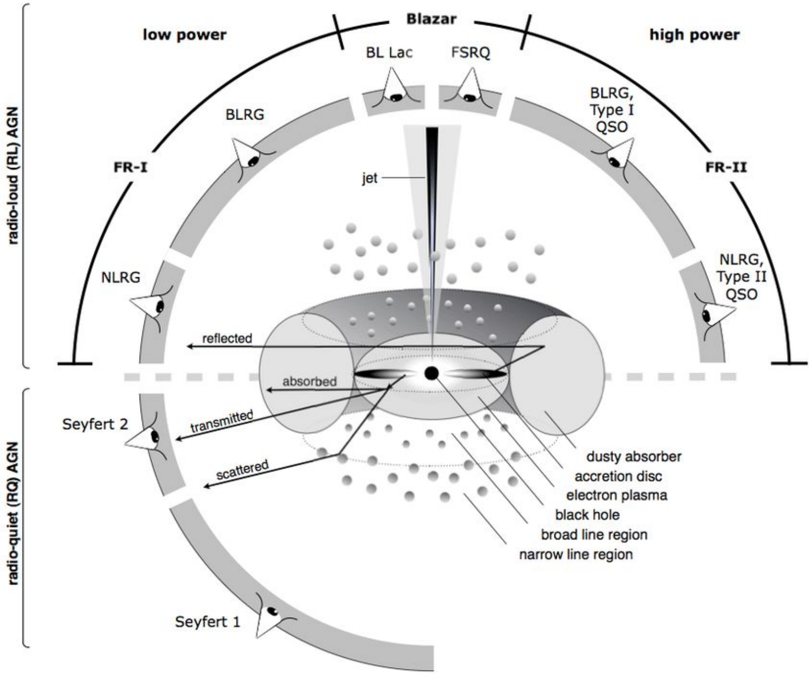

Beckmann & Shrader (2012)

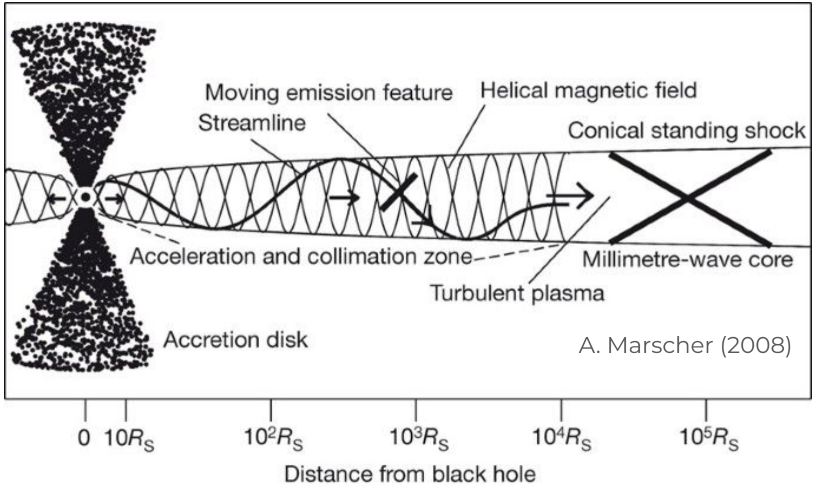

A. Marscher (2008)

- Linear polarization of the synchrotron emission is our most direct probe of the magnetic field geometry in the jet.
- The EVPA direction in the jet frame is perpendicular to the projection of the magnetic field onto the sky.

Factors affecting blazar optical polarization variability

Internal energy processes:

- shock waves propagating along the jet (Marscher 2008, 2010)
- magnetic reconnection (Kagan 2015; Werner 2018)
- turbulence (Marscher 2014)
- two-component model (Cohen and Savolainen 2020; Villforth 2010)

Geometric effects:

- curved jet structure (Nalewajko 2010)
- changes in jet orientation (rotation, precession, nutation) → variable viewing angle and Doppler factor (Raiteri 2017, 2024; Britzen 2023)

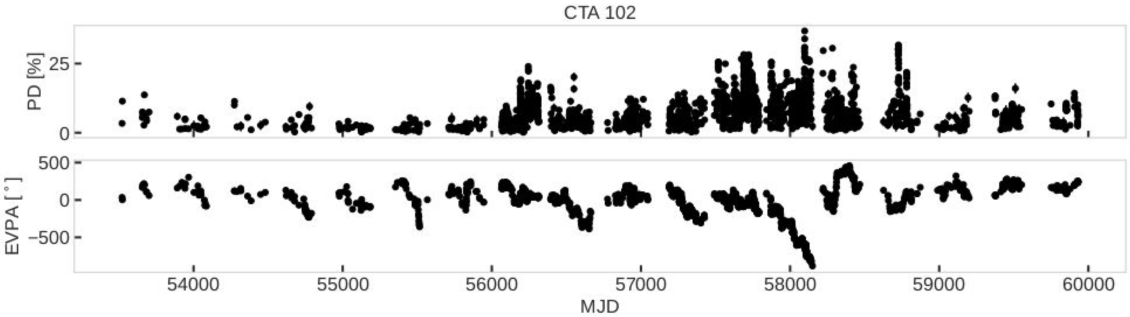

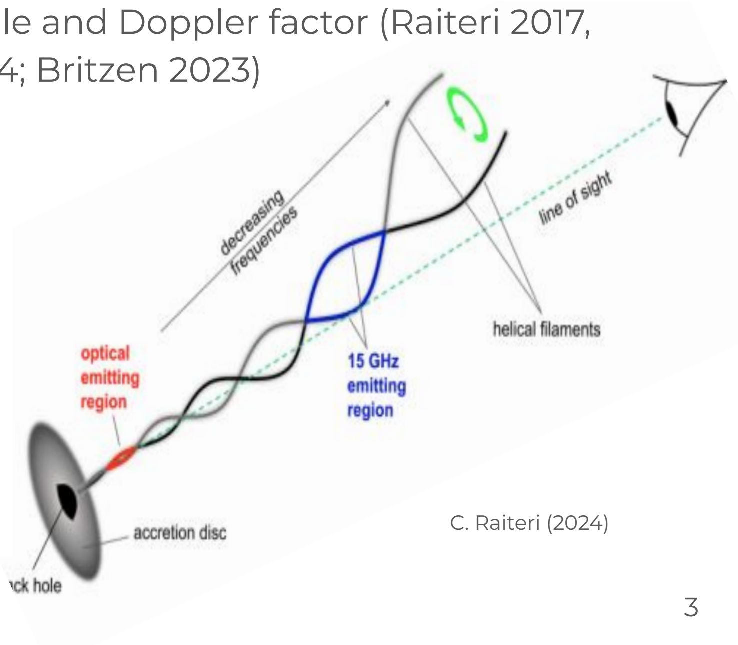

C. Raiteri (2024)

The nπ-ambiguity of the polarization vector (EVPA)

The EVPA, χ, is defined within a 180◦ interval. It's difficult to analyse EVPA variability, since the difference **Δχ = χ2 − χ1 ± nπ** is ambiguous.
To study long smooth variations of EVPA larger than π, the EVPA curve must be reconstructed by resolving this nπ ambiguity between consecutive points under the assumption of **dense, regular sampling**:

$$\chi_{i,\mathrm{adj}} = \chi_i - n\pi \quad \text{with} \quad n = \mathrm{int}\left(\frac{\chi_i - \chi_{i-1}}{\pi}\right)$$

It's a standard procedure
(see Kiehlmann et al. 2016 for details)

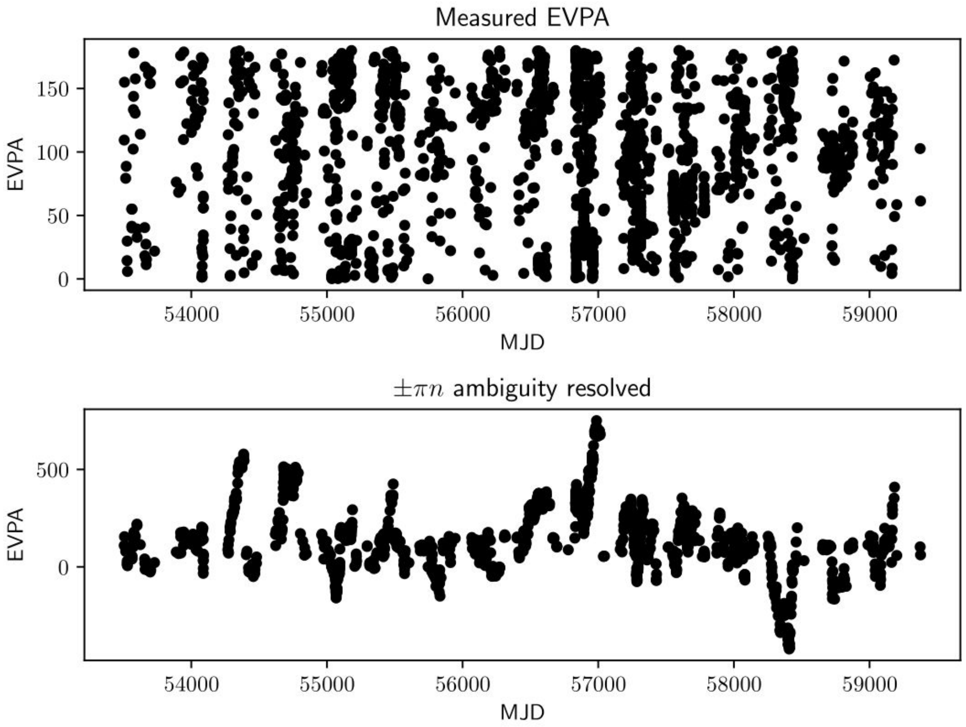

Electric Vector Position Angle (EVPA) rotations

EVPA rotation – ordered EVPA behavior: smooth variations, sometimes quite prolonged (up to several months) and with large amplitudes (up to hundreds of degrees).

Why study EVPA rotations?

- They can reveal the jet's magnetic field structure and evolution
- Their statistics can distinguish deterministic mechanisms (shocks in a helical field) from stochastic ones (turbulent random walk)
- A preferred rotation direction may reflect the global magnetic field geometry, linked to the rotation of the black hole ergosphere or accretion disk
- Rotations often accompany γ-ray flares, neutrino events and the ejection of new radio knots → a link between optical polarization and high-energy activity

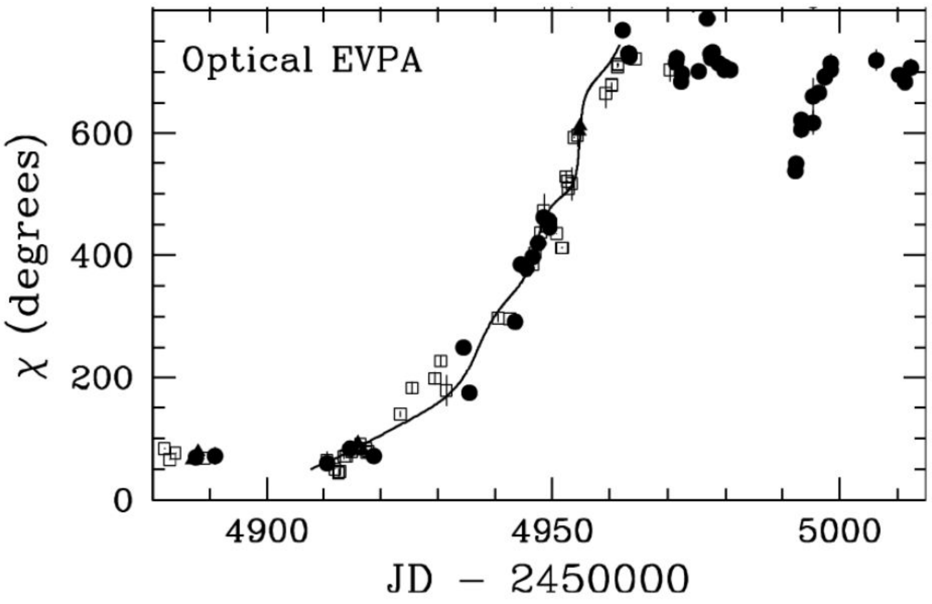

Larionov et al., (2016): PKS 1510

Systematic search for EVPA rotations

- RoboPol program (Blinov et al. 2015, and others)
  - 1st season: 14 rotations in 12 blazars
  - 2nd season: +11 rotations in 10 blazars
  - 3rd season: +13 rotations in 10 blazars
- RINGO2 (Liverpool Telescope) + DIPOL (KVA observatory) (Jermak et al., 2016)
  - over 936 days, 19 rotations were found in 11 out of 15 blazars
- Steward Observatory monitoring program (Otero-Santos et al., 2023)
  - 128 rotations were found over 10 years of monitoring a sample of 26 blazars
- SPBU monitoring program

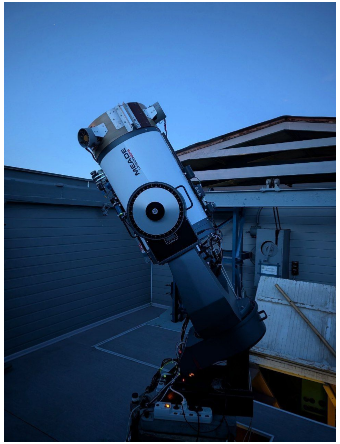

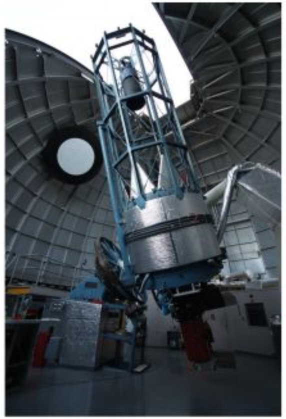

Search for rotations: SPBU monitoring program

- 32 blazars
- Up to 18 years of observations (LX-200, AZT-8, Perkins + Steward archive)
- A new rotation identification method with a statistical significance estimate for each rotation (Savchenko et al. 2024)

1 B1950 name	2 Common name	3 AGN type	4 SED peak classification	5 z	6 δ_{var}	7 Observation period [years]
0219+428	3C 66A	BL Lac	HSP	0.444	12.3 ± 2.8	2005–2021
0235+164	AO 0235+16	HPRQ	LSP	0.940	37.9 ± 5.4	2006–2024
0316+413	3C 84	G	LSP	0.017	~ 6.9	2011–2021
0336-019	CTA 26	HPRQ	LSP	0.852	9.0 ± 4.1	2005–2021
0415+379	3C 111	G	LSP	0.049	2.8 ± 0.2	2006–2021
0420-014	PKS 0420-01	HPRQ	LSP	0.914	25.2 ± 3.4	2005–2023
0528+134	PKS 0528+134	HPRQ	LSP	2.060	17.3 ± 2.4	2007–2022
0716+714	S5 0716+71	BL Lac	ISP	0.310	23.3 ± 3.6	2005–2023
0735+178	PKS 0735+17	BL Lac	LSP	0.424	23.3 ± 3.6	2005–2023
0827+243	OJ 248	LPRQ	LSP	0.939	10.8 ± 1.4	2007–2023
0829+046	OJ 049	BL Lac	LSP	0.174	19.6 ± 6.0	2007–2023
0836+710	Q 0836	LPRQ	LSP	2.172	13.5 ± 0.7	2008–2024
0851+202	OJ 287	BL Lac	LSP	0.306	6.4 ± 1.9	2005–2023
0954+658	S4 0954+65	BL Lac	LSP	0.368	9.8 ± 1.6	2005–2023
1101+384	MKN 421	BL Lac	HSP	0.030	~ 65.5	2006–2022
1156+295	Q 1156	HPRQ	LSP	0.729	15.0 ± 2.8	2005–2024
1219+285	W Com	HPRQ	ISP	0.102	4.5 ± 1.1	2005–2023
1222+216	PKS 1222	FSRQ	LSP	0.435	7.0 ± 0.6	2007–2023
1226+023	3C 273	LPRQ	LSP	0.158	3.2 ± 0.3	2005–2021
1253-055	3C 279	HPQ	LSP	0.536	8.2 ± 0.9	2005–2021
1308+326	B2 1308+32	FSRQ	LSP	0.998	18.5 ± 2.9	2009–2022
1510-089	PKS 1510-08	HPRQ	LSP	0.360	37.0 ± 2.7	2005–2022
1553+113	PG 1553+113	BL Lac	HSP	0.360	~ 1.4	2012–2023
1611+343	Q 1611	LPRQ	LSP	1.401	25.7 ± 3.9	2005–2023
1633+382	Q 1633	HPRQ	LSP	1.814	23.8 ± 3.9	2005–2023
1641+399	3C 345	HPRQ	LSP	0.593	13.2 ± 1.7	2005–2021
1652+398	MKN 501	BL Lac	HSP	0.034	~ 31.5	2007–2023
1749+09	OT 081	BL Lac	LSP	0.320	12.2 ± 1.9	2009–2023
1959+650	Q 1959	BL Lac	HSP	0.047	~ 30.3	2008–2023
2200+420	BL Lac	BL Lac	LSP	0.069	4.3 ± 1.2	2005–2023
2230+114	CTA 102	HPRQ	LSP	1.037	37.5 ± 6.7	2005–2022
2251+158	3C 454.3	FSRQ, HPQ	LSP	0.859	28.8 ± 2.2	2005–2021

Rotation completeness criterion

A rotation is “complete” if its start and end are directly covered by observations: the possible missed EVPA change on each side is < 25% of the total amplitude $\Delta\chi$.

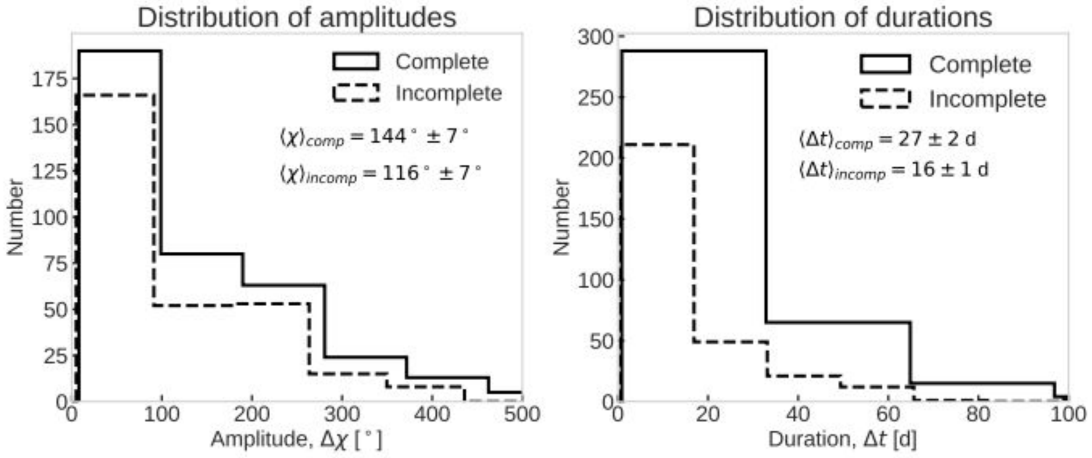

Fig. 2. Distributions of amplitudes (on the left panel) and durations (on the right panel) of 381 complete and 298 incomplete rotations. Each graph contains the average values for complete and incomplete rotations.

Results: the rotation population

- **679 rotations** in 31 of 32 blazars over up to 18 years — the largest uniform sample to date
- 381 rotations are complete (we can analyse their amplitudes and durations)
- Rotations occur in both blazar subclasses: 372 in BL Lacs and 306 in FSRQs
- Rotation amplitude anticorrelates with the mean polarization degree during the rotation (→ next slide)
- 5 sources show a tendency to have a preferred rotation direction; 18 objects show chains of consecutive rotations
- For approximately one-third of the sample, it was shown that the mean direction of the optical polarization position angle is in good agreement with the radio jet position angle
- No significant differences in rotations parameters between BL Lacs and FSRQs were found

Shishkina et al. 2026 (in prep.)

Relationship between rotation amplitude and mean polarization degree during rotation

Fig: Amplitude vs mean PD of each observed **complete** rotation (217 in BL Lacs and 163 in FSRQs).

Main conclusion: there is a clear anticorrelation between the amplitude of the EVPA rotation and the mean value of PD during this rotation.

The one-sided permutation Spearman p-value = 5 · 10−5 corresponds to a Gaussian-equivalent significance of ≈ 3.9σ. This trend is present in both BL Lacs and FSRQs. These results imply that low-amplitude rotations are a distinct and meaningful part of the rotation population that cannot be discarded.

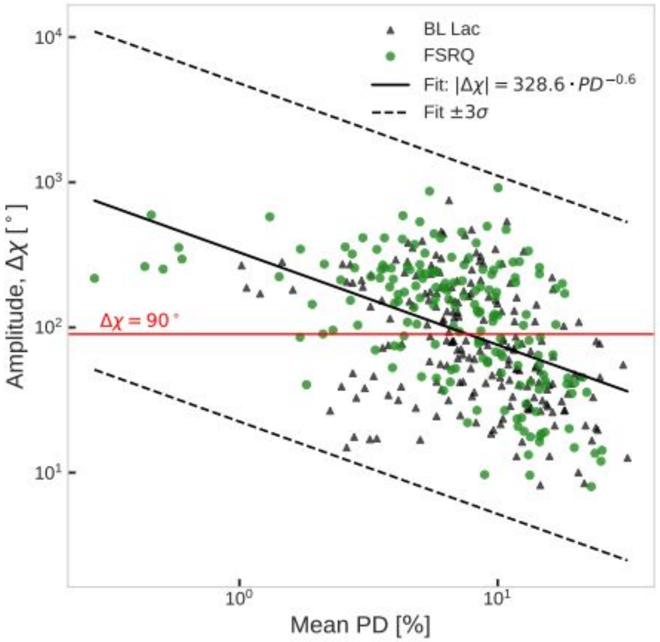

Blazars with a preferred rotation direction

Object	Type	SED peak classification	Number of rotations		σ
OJ 287	BL Lac	LSP	84	30 ↺	2.75
				54 ⟳	
S5 0716+71	BL Lac	ISP	77	**47 ↺**	2.12
				30 ⟳	
3C 454.3	FSRQ, HPQ	LSP	50	**33 ↺**	2.41
				17 ⟳	
CTA 102	FSRQ, HPQ	LSP	31	9 ↺	2.43
				22 ⟳	
PG 1553+113	BL Lac	HSP	14	**12 ↺**	2.75
				2 ⟳	

Shishkina et al. 2024, A&AL

For some blazars the mean direction of the EVPA is in good agreement with the radio jet position angle

1 Common name	2 $\langle\Theta_{jet}\rangle$ (deg)	3 $EVPA_{pref}$ (deg)	4 $\langle PD_{out}\rangle$ [%]
3C 66A	−169.6 ± 5.5	−174.4 ± 0.6	10.6 ± 0.1
AO 0235+16	54.7 ± 6.8	Uniform	14.0 ± 0.3
S5 0716+71	24.3 ± 3.9	Uniform	8.9 ± 0.1
PKS 0735+17	78.5 ± 10.7	Uniform	10.5 ± 0.2
OJ 287	−24.1 ± 1.2	−33.6 ± 0.7	14.7 ± 0.2
S4 0954+65	−13.7 ± 2.1	Uniform	13.2 ± 0.2
MKN 421	−14.4 ± 14.2	−7.1 ± 1.0	3.7 ± 0.1
W Com	106.2 ± 10.6	69.1 ± 1.0	9.6 ± 0.2
PG 1553+113	∼ 50	Uniform	5.1 ± 0.1
MKN 501	119.7 ± 11.8	131.8 ± 0.5	2.3 ± 0.0
OT 081	−1.2 ± 2.3	Uniform	11.5 ± 0.3
Q 1959	127.9 ± 12.9	–*	3.9 ± 0.1
BL Lac	−170.0 ± 1.8	−163.3 ± 0.4	9.1 ± 0.1
CTA 26	78.7 ± 4.6	Uniform	8.5 ± 0.3
PKS 0420-01	121.0 ± 3.7	Uniform	11.8 ± 0.4
PKS 0528+134	64.8 ± 6.0	–*	5.8 ± 0.5
OJ 248	127.1 ± 5.8	Uniform	1.7 ± 0.1
OJ 049	63.1 ± 5.7	–*	10.2 ± 0.2
Q 0836	−140.0 ± 3.3	–*	2.8 ± 0.1
Q 1156	10.0 ± 3.8	Uniform	12.7 ± 0.2
PKS 1222	23.5 ± 1.9	−1.3 ± 0.7	5.8 ± 0.1
3C 273	−141.3 ± 0.7	−131.9 ± 1.5	0.4 ± 0.0
3C 279	−152.7 ± 1.0	−126.1 ± 1.1	14.7 ± 0.2
B2 1308+32	−64.9 ± 4.7	–*	14.3 ± 0.6
PKS 1510-08	−33.1 ± 2.8	Uniform	4.6 ± 0.1
Q 1611	163.3 ± 3.3	–*	3.1 ± 0.1
Q 1633	−51.6 ± 6.1	−7.3 ± 1.4	8.3 ± 0.2
3C 345	−100.5 ± 2.6	−120.2 ± 2.0	6.9 ± 0.2
CTA 102	130.9 ± 3.6	Uniform	8.1 ± 0.2
3C 454.3	−81.8 ± 1.6	Uniform	6.2 ± 0.1
3C 84	173.3 ± 0.4	–*	1.5 ± 0.0
3C 111	66.1 ± 2.2	−53.4 ± 1.3	4.0 ± 0.2

Summary

- EVPA rotations are a common phenomenon in blazars — and a direct probe of the magnetic field structure of their jets.
- Rotations can be generated by both deterministic and stochastic mechanisms. At the same time, the influence of geometric effects cannot be excluded.
- A preferred rotation direction may reflect the global magnetic field structure, related to the rotation of the black hole ergosphere or accretion disk (Semenov 2004).
- Rotations may be associated with γ-ray flares (this suggests their co-spatial origin) and the appearance of new knots on radio maps.
- Since the regions of optical and radio emission generation are different, jet-frame interpretations require caution.

Thank you for your attention!

Additional slides

EVPA rotations in terms of QU-plane

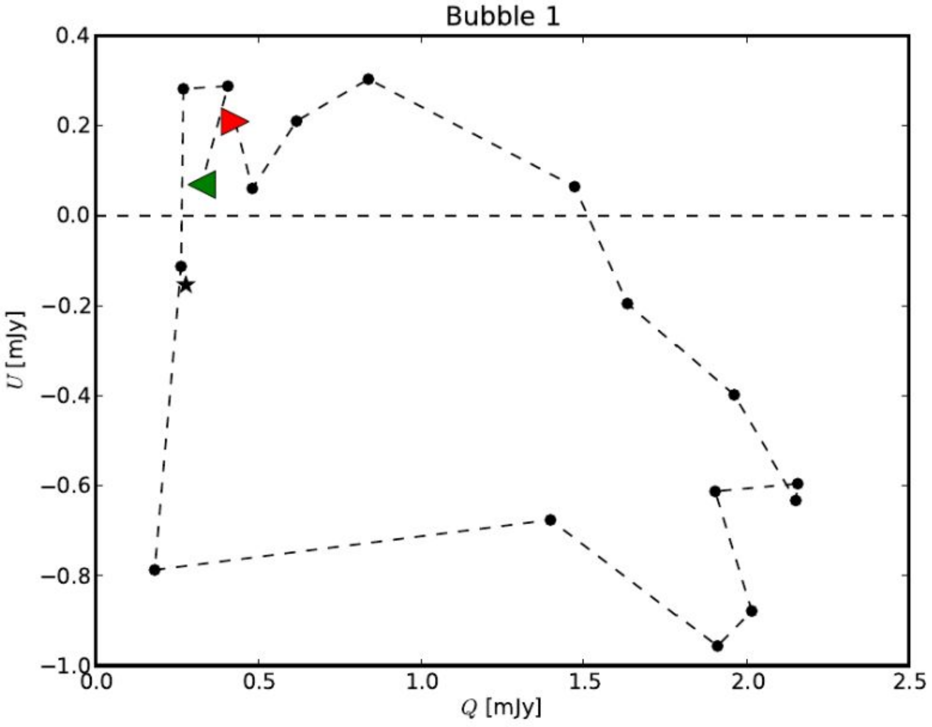

Villforth et al., (2010): OJ 287

Rotation completeness criterion

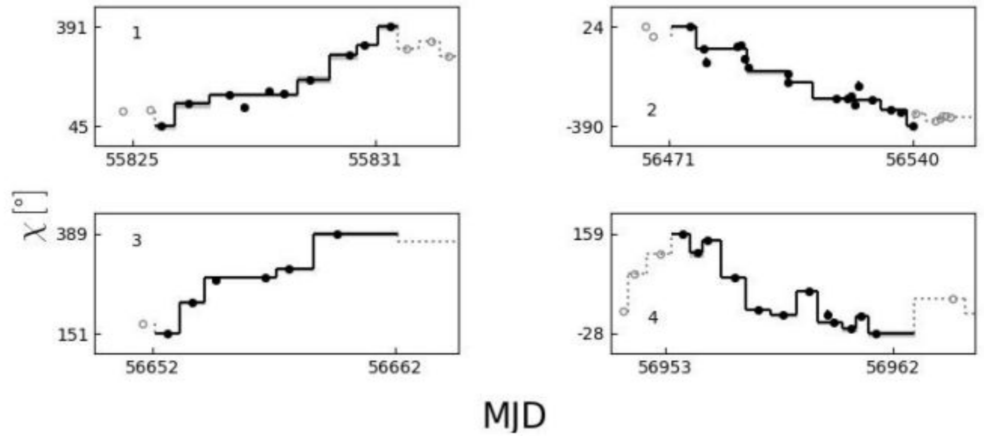

Fig. 1. Example of the differences between complete (1, 2) and incomplete rotations (3, 4) in the CTA 102.

We defined the following values: Δt1 is the time between the first observational data point of the rotation and the previous observational data point. Similarly, Δt2 is the time between the last observational data point of the rotation and the following observational data point after the rotation. The corresponding changes of the EVPA are Δχ1 = Δt1 · ṽ and Δχ2 = Δt2 · ṽ, where ṽ is the mean rotation rate.

We define a complete rotation as a rotation with both Δχ1 and Δχ2 lower than 25% of the total observed amplitude of the rotation Δχ. This restriction imposes an upper limit on the underestimation of the total amplitude and the total duration of the rotation regardless of its mean rate. Rotations that do not satisfy this criterion are called "incomplete".

Analysis of rotation parameters

For the entire rotation sample

Weighted mean over the object sample
(each object has equal weight regardless of the number of detected rotations)

Rotation parameters

Table 2. Properties of the observed rotations.

1	2	3	4	5	6	7	8	9	10
Subclass	$N_{\text{rotations}}$	$\langle\Delta\chi\rangle$[°]	$\langle\Delta t_{\text{obs}}\rangle$[d]	$\langle\Delta t_{\text{jet}}\rangle$[d]	$\langle\overline{v_{\text{obs}}}\rangle$[°/d]	$\langle\overline{v_{\text{jet}}}\rangle$[°/d]	S_{norm}	f_{obs}	f_{jet}
BL Lacs	206	105.5 ± 15.8	26.5 ± 2.8	441.6 ± 118.9	6.9 ± 1.5	1.0 ± 0.4	1.1 ± 0.1	1.8 ± 0.4	0.3 ± 0.1
FSRQs	174	165.1 ± 23.6	34.0 ± 3.5	357.1 ± 73.6	7.7 ± 1.0	0.9 ± 0.1	1.5 ± 0.2	1.0 ± 0.2	0.1 ± 0.03
LSPs	269	157.9 ± 18.9	32.3 ± 3.0	334.7 ± 55.6	7.7 ± 0.9	1.0 ± 0.2	1.13 ± 0.2	1.2 ± 0.3	0.2 ± 0.1
ISPs	55	138.6 ± 32.3	25.6 ± 3.0	259.6 ± 142.6	10.7 ± 6.5	1.0 ± 0.02	1.3 ± 0.2	2.6 ± 1.6	0.2 ± 0.001
HSPs	57	78.7 ± 20.5	30.8 ± 5.1	697.5 ± 242.3	3.9 ± 1.5	0.7 ± 0.6	1.1 ± 0.2	1.3 ± 0.4	0.3 ± 0.2

Main conclusion: the observed differences disappear when transitioning to the jet frame. This may mean that the differences are mainly due to different Doppler factors and differences between individual sources.
Difference from other works: in Otero-Santos 2023, rotations were considered in the observer's frame.

$$\Delta T_{\text{jet}} = \Delta T_{\text{obs}} \frac{\delta}{1+z}.$$

Rotation observation frequency

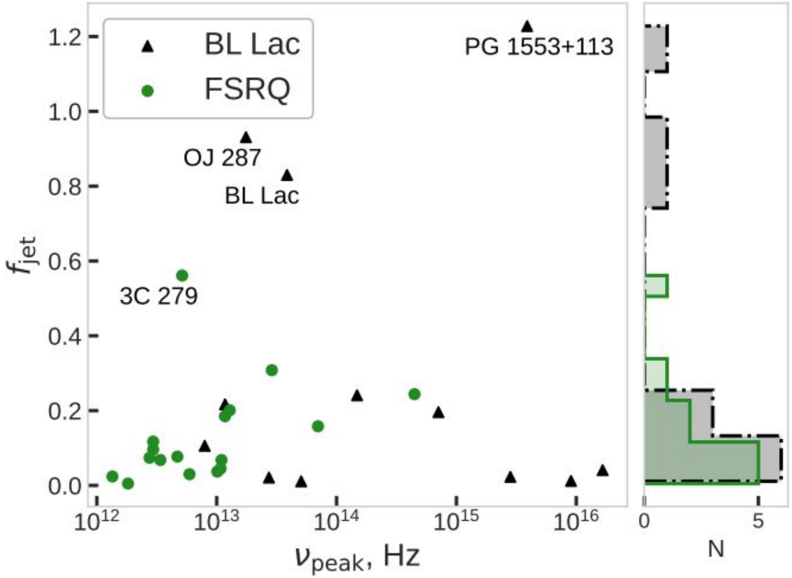

Fig. 4. The dependence of the jet-frame rotation occurrence frequency f_{jet} on the synchrotron peak frequency ν_{peak}, with BL Lacs indicated by black triangles and FSRQs indicated by green dots.

$$\Delta T_{jet} = \Delta T_{obs} \frac{\delta}{1+z}.$$

Polarization degree

Class	Mean polarization degree during rotations	Mean polarization degree outside rotations
FSRQ	8.0 ± 1.0%	7.3 ± 1.0%
BL Lac	8.2 ± 1.2%	9.0 ± 1.3%
LSP	8.40 ± 0.91%	8.35 ± 0.93
HSP	5.15 ± 1.68%	5.12 ± 1.45

Comparison with other works:

- when calculating mean values of polarization degree and angle in a source, we exclude rotation periods (both complete and incomplete)
- we do not find a consistent tendency for the polarization degree to decrease during rotations

Chains of rotations

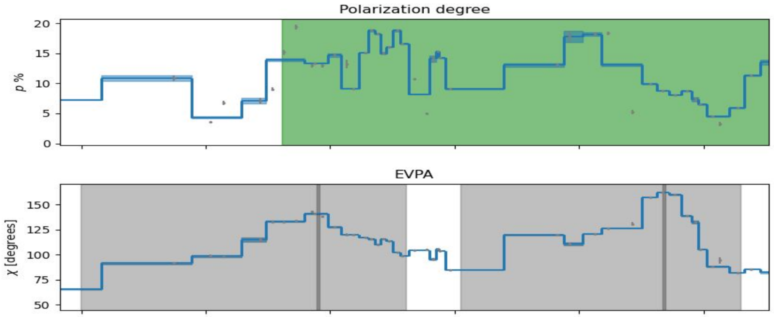

OJ 287
MJD 57080 - MJD 57130

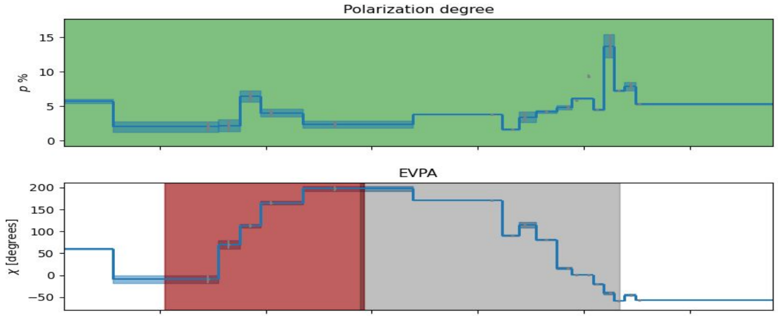

PKS 1510
MJD 57615 - MJD 57640

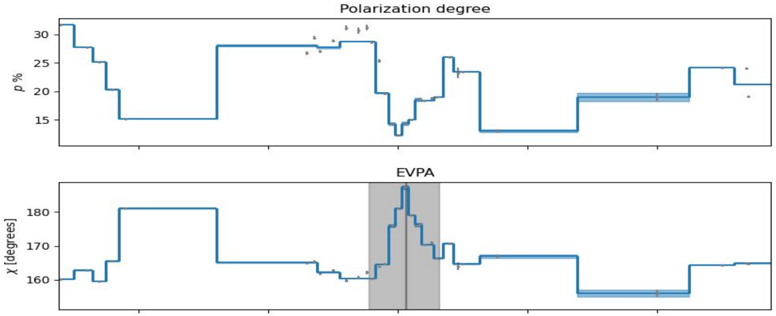

OJ 287
MJD 54750 - MJD 54790

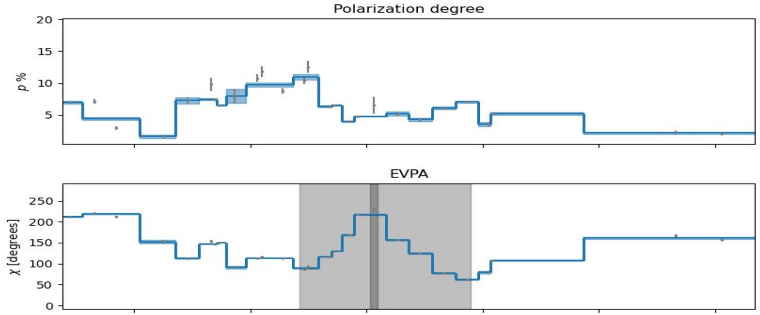

S5 0716
MJD 57510 - MJD 57535

Why do chains of rotations occur?

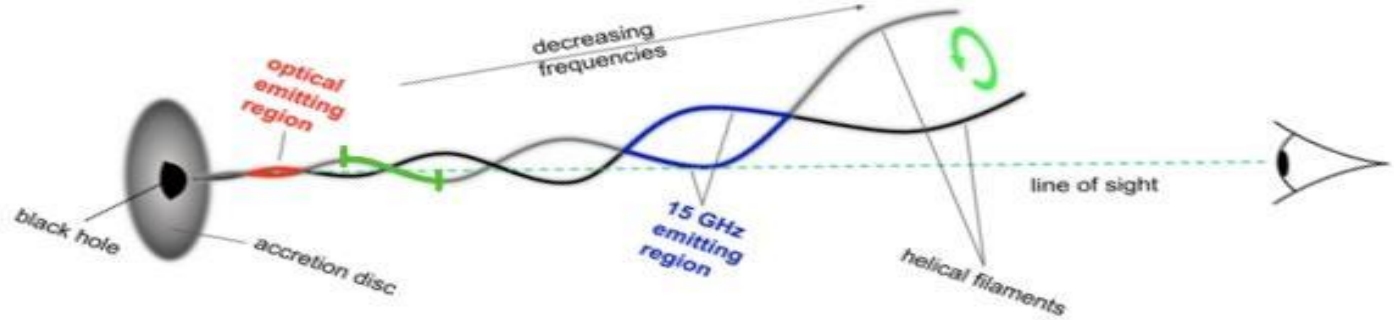

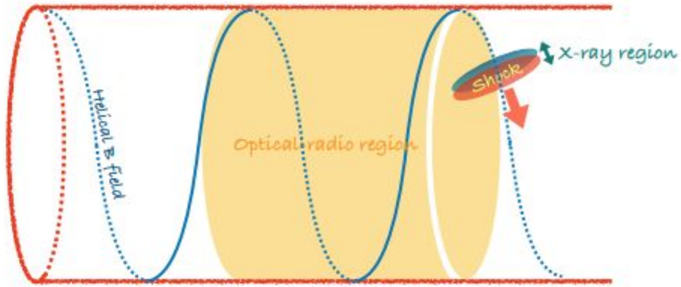

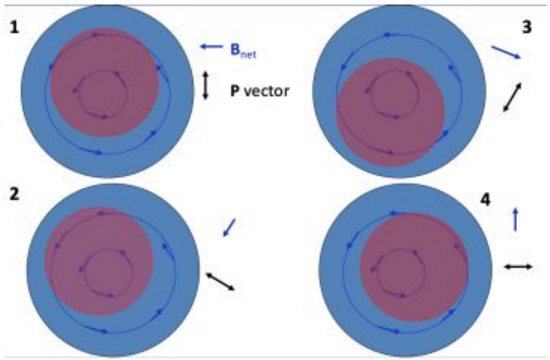

C. Raiteri (2024), L. Gesu (2023)